New Journal and we have not received input yet 34 (2022) 101368

Contents lists available at ScienceDirect

Thermal Science and Engineering Progress

journal homepage: www.sciencedirect.com/journal/thermal-science-and-engineering-progress

Heat transfer and performance enhancement investigation of novel plate heat exchanger

Ahmad Aboul Khail [a,1,*], Ali Erişen [b]

[a] Department of Mechanical Engineering, Hasan Kalyoncu University, Gaziantep 27010, Turkey
[b] OSTİM Technical University, OSTİM, Yenimahalle, Ankara, Turkey

ARTICLE INFO

Keywords:
Novel plate heat exchanger
Longitudinal turbulence
Transverse turbulence
Coefficient of friction
Hyperbolic tangent function
Nusselt number
Performance

ABSTRACT

In this paper, the enhancement of heat transfer and performance have been investigated numerically for a novel plate heat exchanger. The effect of changing the shape of the hyperbolic tangent function and the dimensions of the plate profile on the flow properties have been studied numerically by ANSYS Fluent 16.0. The results show that the transverse disturbances of fluid movement increase the heat transfer, as the heat transfer is enhanced by increasing the concavity of the hyperbolic tangent function. Moreover, as the corrugation depth of the plate increases, the heat transfer increases. As a result, it was found that the effect of the longitudinal turbulence in the direction of flow on the heat transfer is greater than the effect of the transverse turbulence. By comparing the results with those of the novel plate heat exchanger, it was shown that the heat transfer and performance have been enhanced on average by 13% and 8%, respectively when using the hyperbolic tangent function "y = tanh (x)", while they have been enhanced on average by 52% and 36% respectively at the corrugation depth of 2.5 mm. Further, when comparing the enhanced performance of the novel plate heat exchanger with those of other plate geometries, the enhanced performance showed an improvement of up to 37% over its nearest competitor.

1. Introduction

The increasing need to improve heat transfer and performance in plate heat exchangers PHEs has become an important source of inspiration for both researchers and producers to meet the increasing needs of industry requirements in addition to reducing energy consumption and harmful emissions to the environment. Within this concept, several researchers have undertaken researches to study the flow properties of the conventional chevron type plate heat exchanger CPHE. Moreover, others have suggested using modified or new plate geometries and hybrid fluids to increase heat exchange and performance. Luan designed a PHE's plate geometry with longitudinal and transverse ripples Luan et al. [14]. The effect of corrugation shape on the characteristics of the flow was investigated [20]. In another study, the chevron angle effect on the heat exchange was examined Giurgiu et al. [5]. Zhang proposed a new plate shape represented by convex and concave half capsules Zhang et al. [21]. The effect of the geometrical parameters of the chevron type plates on the pressure drop in PHEs was studied Wang et al. [19]. The effect of plate corrugation geometry on the performance of PHEs exposed to fouling was investigated (Li, [13], Matsegora et al. [15]. Moreover, a numerical study has been carried out on the effect of the number of plates and flow distribution on the performance of the PHE [18]. To improve the heat transfer properties of the flat and CPHE, several studies have been carried out through geometrical modifications to the fluid path within the flow path [6–9]. Afshari et al. have studied the effect of the number of plates and the use of hybrid nanofluids on the performance of the plate heat exchanger numerically and experimentally, showing an increase in heat exchange compared to the use of nanofluids only, when using a different number of platesAfshari et al. [2]. Mohebbi's numerical study confirmed that increasing the ripple depth increases the heat exchange in the plate heat exchanger [17,16]. In order to improve the performance and the heat exchange of PHE, a novel plate geometry has been proposed based on a repeating basic unit with a half-ellipse cross-section corrugates according to the hyperbolic tangent function HTF (y = tanh(x/2)) [1].

In this paper, and as a follow-up to the aforementioned research [1], the enhancement of the heat transfer and performance of the novel plate heat exchanger NPHE is investigated by studying numerically the effect of changing depth and surface of ripple (hyperbolic tangent function formula(on the flow characteristics (Nu number, friction coefficient, and performance) within the range of Reynolds number (500–5000). The

* Corresponding author.
E-mail addresses: khailnuc@gmail.com (A. Aboul Khail), ali.erisen@ostimteknik.edu.tr (A. Erişen).
[1] Ahmed Sadık is the second name of the author Ahmad Aboul Khail due to his dual nationality.

https://doi.org/10.1016/j.tsep.2022.101368
Received 3 December 2021; Received in revised form 25 April 2022; Accepted 7 June 2022
Available online 25 June 2022

Nomenclature

d_h	Hydraulic diameter (m)
f	Friction coefficient
A_f	Flow cross-sectional area (m^2)
h	Convective heat transfer coefficient ($W/m^2.K$)
$\dot{m}$	Mass flow rate (kg/s)
Nu	Nusselt number
p	Perimeter of wet cross section (m)
Re	Reynolds number
T	Temperature (K)
$\overline{u}$	Average velocity (m/s)
$\overline{q}$	Average heat flux (W/m^2)
p	Pressure (N/m^2)
v	Velocity (m/s)

Greek alphabet

λ	Thermal conductivity (W/m.K)
μ	Dynamic viscosity (kg/m.s)
ρ	Density (kg/m^3)
α	Thermal ddiffusivity (m^2/s)
τ	Shear stress (N/m^2)

Subscripts

f	Fluid
w	Wall

results indicate that both heat transfer and performance are enhanced at remarkable rates compared to those attributed to the novel plate heat exchanger. Moreover, comparing the enhanced heat transfer and performance with those of other plate geometries in the literature showed a significant improvement.

2. Numerical simulation

2.1. Geometrical model

Enhancing heat transfer and performance in most research is addressed either by modifying the traditional chevron plate geometry or by proposing new plate geometries for PHE. In both cases, many of the results of these researches lead to an enhancement of heat transfer at the expense of a significant increase in the value of the coefficient of friction, or vice versa. In this research, as a result of investigating the enhancement of heat transfer and performance through changing specific parameters affecting the flow structure, it was found that the heat transfer can be enhanced well with a small increase in the friction coefficient, which is positively reflected in the performance value.

The geometry of the plate ripples plays a key role in shaping the fluid flow patterns within the heat exchanger and thus affects the thermo-hydraulic flow characteristics. Therefore, in NPHE the HTFs were chosen for the undulations of the geometric plate, which is characterized by a smooth change in its concavity that increases the transverse turbulence of the fluid without causing a noticeable increase in the coefficient of friction [1]. Fig. 1a represents the plate geometry used in the NPHE where the base unit of the plate is formed according to HTF ($y = \tanh(x/2)$; $x \in [-2.5, +2.5]$) and a cross-section as a half ellipse (Fig. 1b). By mirror this shape towards the × and z axes according to the desired dimensions, the final shape of the plate is obtained (Fig. 1c). For more details on the geometric model of the novel plate, see article [1]. The HTF "$y = \tanh(x/2)$" is mainly responsible for the transverse turbulence of the fluid (in the direction of the x-axis). It is understood from this that any change in the formula of this function will affect the transverse turbulence that contributes to the mixing of the fluid and thus affects the heat exchange. Fig. 2 shows the graphs of each HTFs: tanh(x), tanh(x/2), tanh(x/3) respectively. Also, according to the same order, the surface area of each curve with the x-axis within the [-2.5, +2.5] domain equals 3.627, 2.543, and 1.8792, respectively. On the other hand, the dimensions of the ellipse are the prominent parameter to examine the effect of change the corrugation depth of the plate on the flow properties. Fig. 1-b shows the dimensions of the cross-section of the profile of the basic unit forming the plate, where a represents the radius of the ellipse in the direction of the axis z, and b represents the radius of the ellipse in the direction of the axis y, which also represents the corrugation depth of the plate. Three values for each of a and b were chosen to be studied as follows: (a = 3 mm, b = 2 mm), (a = 4 mm, b = 1.5 mm), (a = 2.4 mm, b = 2.5 mm). These values are chosen so that the area of the ellipse remains constant ($\pi ab = 6\pi$). The base case studied previously represented both the HTF (tanh(x/2)) and the dimensions of ellipse (a = 3 mm, b = 2 mm) [1]. In this paper, the effect of changing the HTF with the constancy of the ellipse dimensions at (a = 3 mm, b = 2 mm), and the ellipse dimensions with the constancy of the HTF at the formula "tanh (x/2)" will be studied on the flow characteristics.

2.2. Calculation domain and boundary conditions

In this paper, the calculation domain is adopted in the form of a tape from the heat transfer region of the plate with a width of 10 mm (representing the width of two basic units). The calculation domain consists of an opposite flow of hot and cold fluids separated by the aforementioned plate tape as shown in Fig. 3. Accordingly, the symmetry condition is taken as the boundary condition at both ends of this strip as shown in Fig. 3. The entry temperatures of both hot and cold water were set at 50 °C and 14 °C respectively. At the outlets of both cold and hot water, the pressure has been set as 5 bar. The boundary conditions at the upper and lower surfaces are adopted as adiabatic walls and there is no slip. The turbulence intensity and turbulence viscosity ratio at the inlets for all Reynolds numbers are set to 5% and 10 respectively. The aforementioned boundary conditions are the same for all the studied cases and agree to the boundary conditions in [1], the boundary condition for the mass flow rates in the hot and cold water inlets differs numerically from one studied state to another, in all cases, the mass flow rates of the hot and cold fluid mass are the same.

The properties of the working fluid (water) and the plate of NPHE used in the numerical study are shown in Table 1.

2.3. Methods and assumptions

The SIMPLE algorithm to unravel the (p–v) coupling was adopted. For the spatial discretization, the second-order upwind scheme for the momentum and for pressure the standard scheme and TKE (turbulent kinetic energy), energy equations, and the dissipation rate were adopted. With respect to residuals, for continuity and velocity equations they were set to 10^{-3}, while for the energy equation were set to 10^{-6}. As for the relaxation factors, they were adopted to obtain the convergent solution as follows: for energy and turbulent viscosity 0.9, for the specific dissipation rate and turbulent kinetic energy 0.8, body forces and density 0.9, and for momentum and pressure 0.3. In the solution initialization section, the initial values resulting from the standard initialization method calculated at the cold water inlet were adopted. In order to facilitate the numerical modeling procedure, the working fluids were considered incompressible and their physical properties are constant. Moreover, both the effect of gravity and the transfer of heat by radiation were neglected. The plate between the cold and hot water is made of steel with a thickness of 0.6 mm and has constant properties. The flow in CPHEs is generally turbulent at $Re > 400$ Gherasim et al. [4]. Moreover, it has been proven that in this novel type of PHE, within the studied range (500–5000) the flow is turbulent [1]. Therefore, the flow was considered in this study to be steady and turbulent. Because the Shear Stress Transport (SST) k-ω turbulence model combines the

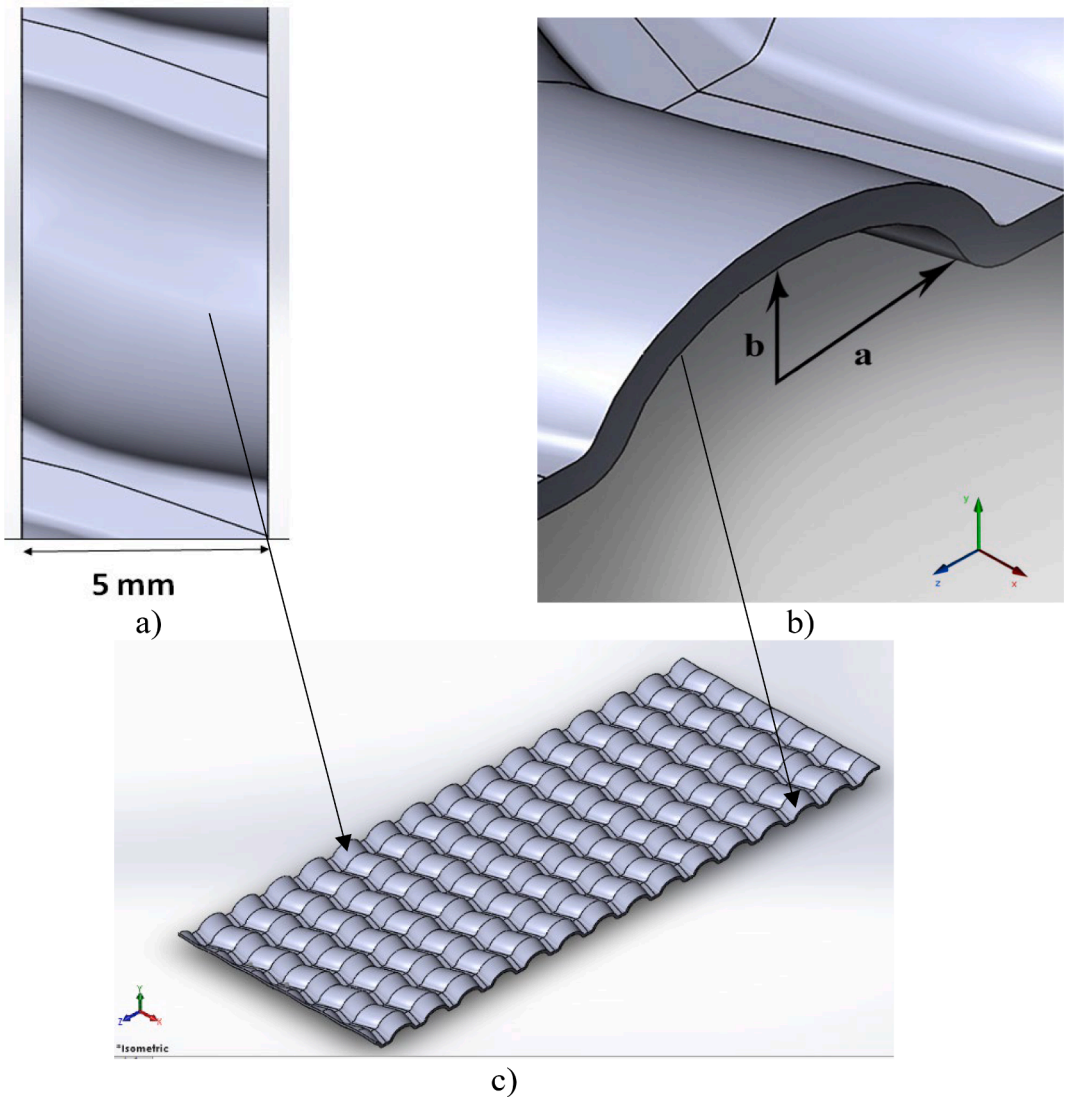

Fig. 1. Formation of the novel plate. a) The elementary unit of the plate. b) The side view of the plate. c) The novel plate [1].

advantages of both k-ω and k-ε models Kanaris et al. [11], SST k-ω as turbulence model was adopted in this study. According to the assumptions mentioned above, the equations governing the study of this flow are according to the following:

The equation of Continuity:

$$\frac{\partial u_x}{\partial x}+\frac{\partial u_y}{\partial y}+\frac{\partial u_z}{\partial z}=0 \tag{1}$$

The equation of Momentum:

$$u_x\frac{\partial u_i}{\partial x}+u_y\frac{\partial u_i}{\partial y}+u_z\frac{\partial u_i}{\partial z}=-\frac{1}{\rho}\frac{\partial p}{\partial x_i}+\nu\left[\frac{\partial^2 u_i}{\partial x^2}+\frac{\partial^2 u_i}{\partial y^2}+\frac{\partial^2 u_i}{\partial z^2}\right];i=x,y,z \tag{2}$$

As for energy equation:

$$u_x\frac{\partial T}{\partial x}+u_y\frac{\partial T}{\partial y}+u_z\frac{\partial T}{\partial z}=\alpha\left[\frac{\partial^2 T}{\partial x^2}+\frac{\partial^2 T}{\partial y^2}+\frac{\partial^2 T}{\partial z^2}\right] \tag{3}$$

2.4. Mesh procedures and valiadation

The numerical study was carried out using ANSYS Fluent version 16.0 installed on a computer with 64 GB RAM. The tetrahedral elements unstructured mesh was adopted due to the complex geometry of the flow within the channel. Further, the elements near the wall were condensed to increase the accuracy of numerical modeling results (Fig. 4). In general, there are two methods for testing the independence of the computational grid: the first depends on increasing the mesh size several times and tracking one or more parameters to reach a relatively small change of the tracked parameter Islam et al. [9], and the second method is based on changing the size of the computational grid for one time, within which the change of the tracked parameters in relation to the change in the size of the mesh is small relatively Zhang et al. [21]. In this research, the second method was adopted to conduct a mesh independence test for all cases. Table 2 represents the procedures used to test mesh independence to ensure the reliability of the numerical results. Whereas, for each case, the convective heat transfer coefficient h and the pressure drop ΔP between the inlet and outlet of the fluids for cold water were tracked when increasing the number of elements of each grid for each case from mesh 1 to mesh 2. For example in the case of (y = tanh (x)) when the number of the elements in the computational grid was increased from 10,886,916 to 17,926,622 (about 64%), convective heat transfer coefficient and pressure drop changed (decreasing) by 2.4%, 1.8% respectively. Thus, mesh 1 is chosen to save calculation time and cost. In the same way, the computational grids were adopted for the rest of the other cases. In the case (a = 2.4, b = 2.5) mm, it is mathematically reflected in the relative error in the Nusselt number, the coefficient of friction, and the performance with the values of 2.77%, 6.14%, and

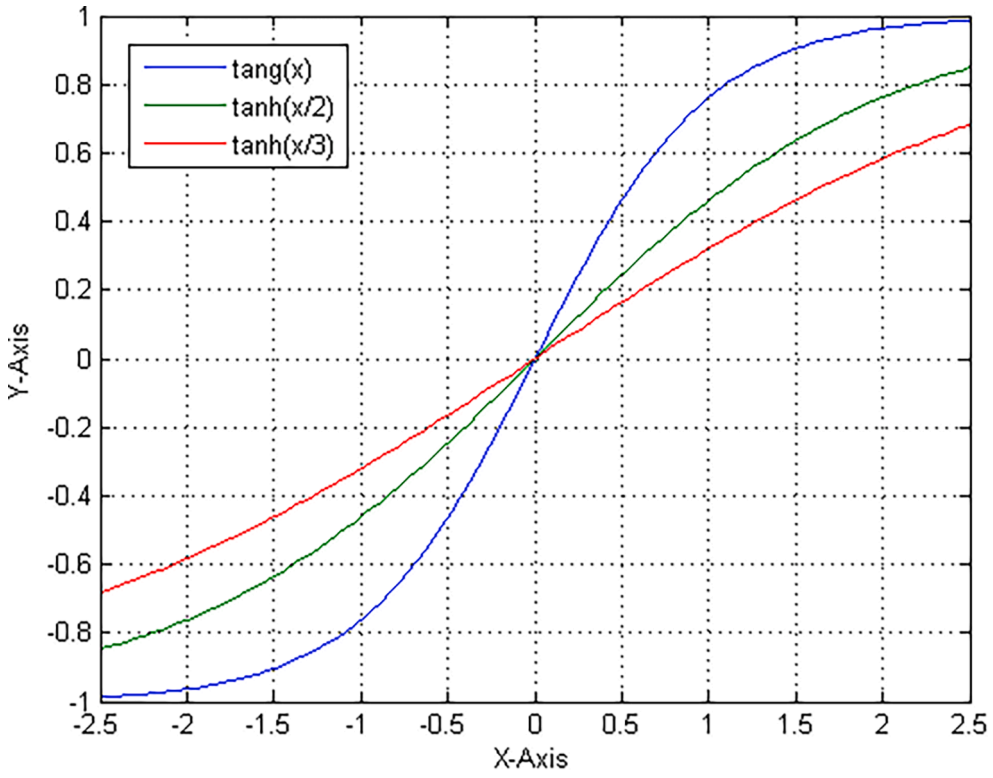

Fig. 2. Different HTFs curves.

4.68%, respectively.

As for the validation of numerical results, the state (tanh(x/2), a = 3 mm, b = 2 mm) was validated by comparing the Nusselt number values resulting from numerical simulation with those from a new analytical method [1]. The maximum difference between the numerical and analytic values did not exceed 3.6% for all Reynolds numbers within the range (500–5000).

2.5. Computation of main parameters

The Reynolds number was calculated for all cases at the entrance to the cold fluid according to the following relationship:

$$Re = \frac{\dot{m} d_h}{\mu . A_f} \tag{4}$$

where $\dot{m}$ the mass flow rate, d_h the hydraulic diameter, μ the dynamic viscosity, and A_f the area of flow cross-sectional. As for the hydraulic diameter, it was calculated from the following relationship:

$$d_h = \frac{4A_f}{p} \tag{5}$$

where p the perimeter of wet cross section. The friction coefficient was calculated from the following relationship:

$$f = \frac{\overline{\tau_W}}{\frac{1}{2}\rho \overline{U}^2} \tag{6}$$

where $\overline{\tau_W}$ the average value of shear stress, $\overline{U}$ the averagevalue of fluid velocity, and ρ the density. The mean Nusselt number values and the mean convective heat transfer coefficient values were calculated as follows:

$$\overline{h} = \frac{\overline{q}}{\overline{T_W} - \overline{T_f}} \tag{7}$$

$$Nu = \frac{\overline{h} d_h}{\lambda_f} \tag{8}$$

where $\overline{q}, \overline{T_W}, \overline{T_f}, \lambda_f$ The mean values of heat flux, wall temperature, fluid temperature, and fluid thermal conductivity, respectively. As for the average value of performance, it is calculated in this research according to the following relationship Fan et al. [3]:

$$Performance(P) = Nu/f^{1/3} \tag{9}$$

3. Rsesults and discussion

3.1. The effect of HTFon the thermal and hydraulic characteristics of flow

The average values of Nusselt number at Reynolds number (500–5000) values were calculated from the results of numerical analysis using Eqs. (7) and (8). Fig. 5 shows the average values of the Nusselt number corresponding to the Re numbers according to the functions y = tanh (x), y = tanh (x/2), and tanh (x/3), respectively. From Fig. 5, it is seen that the flow according to the function "y = tanh (x)" has relatively higher Nusselt numbers than other flows, especially at higher Reynolds numbers. Moreover, the Nusselt number corresponding to the function y = tanh (x) is, on average, about 8 % greater than the Nusselt number corresponding to the closest curve (y = tanh (x/2) [1]. This can be explained by the fact that the concave of the curve y = tanh (x) (see Fig. 2) is greater than that of the other studied functions, in other words, the gradient of the curvature of y = tanh (x) function is greater than that of the other functions. Thus, the plate geometry will further contribute to the transverse turbulence of the fluid flow and increase the fluid mixing and consequently, the heat exchange will increase.

Fig. 6 shows the average values of the friction coefficient corresponding to Re numbers according to the functions y = tanh (x), y = tanh (x/2), and tanh (x/3), respectively.

It can be seen from Fig. 6 that the friction coefficient corresponding to the function y = tanh (x/3) is the lowest compared to the other

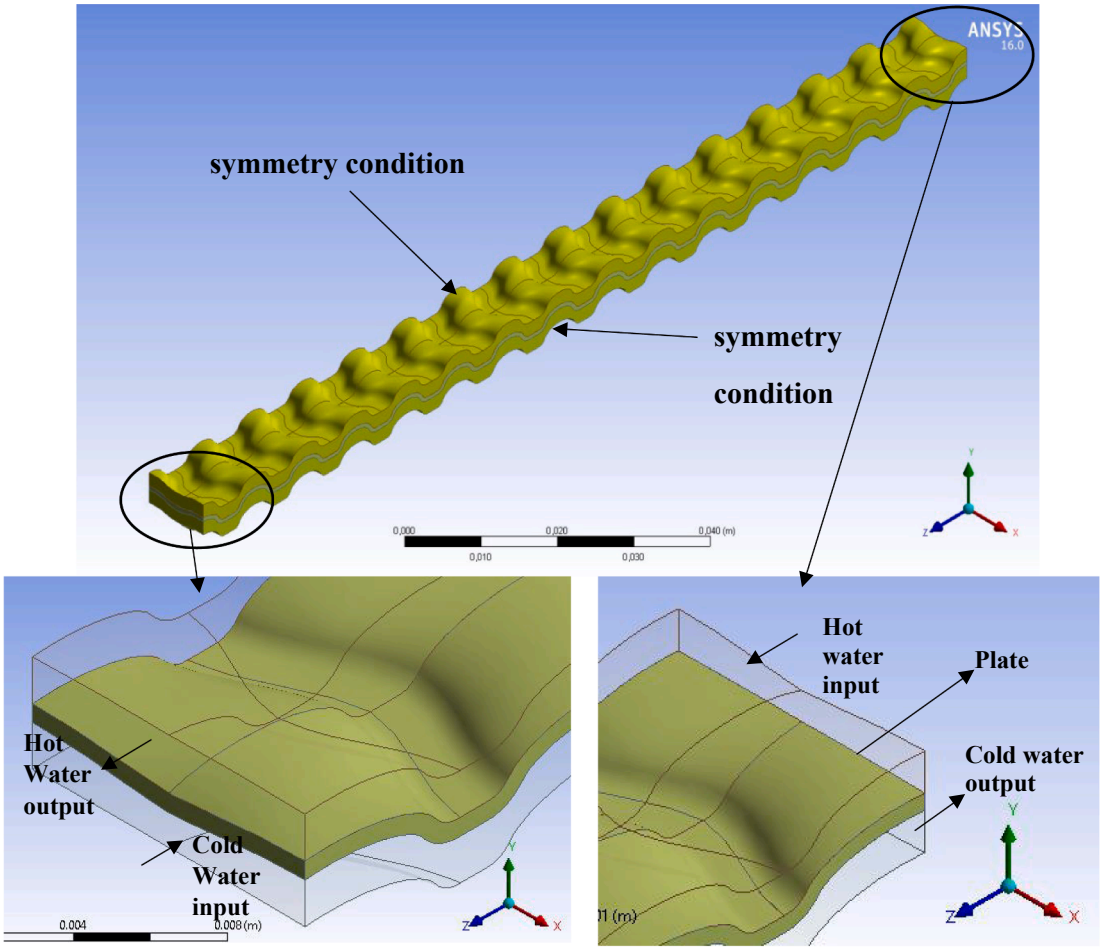

Fig. 3. Calculation domain.

Table 1
The properties of the plate and water used in the numerical study.

Water		Plate	
Viscosity	0.001003 kg/m.s	**Material**	Steel
Density	998.2 kg/m^3	**Thickness**	0.6 mm
Specific Heat	4182 J/(kg.K)	**Density**	8030 kg/m^3
Thermal conductivity	0.6 W/(m.K)	**Specific Heat**	502.48 J/(kg.K)
		Thermal conductivity	16.27 W/(m.K)

investigated functions. This is because this function has less gradient of curvature compared to others and therefore less turbulent effect on the fluid than the effect of other functions. The convergence in the geometrical shape of the surfaces according to the studied functions causes convergence in the hydro-thermal properties of the flow (especially at low Reynolds numbers). As the flow is at the beginning of the turbulence phase (transitional flow), the laws governing the flow differ. On the other hand, the slight difference in the values of shear stress at the wall (resulting from the different gradient of curvature of the studied functions) can lead, in conjunction with the approximations in the numerical study, to such a result. Fig. 7 shows the error bars for Fig. 5 and Fig. 6, respectively.

As for the performance according to the Nu/f$^{1/3}$ parameter, Fig. 8 shows that the flow performance according to the function y = tanh (x) is relatively higher than the other examined functions. Moreover, the

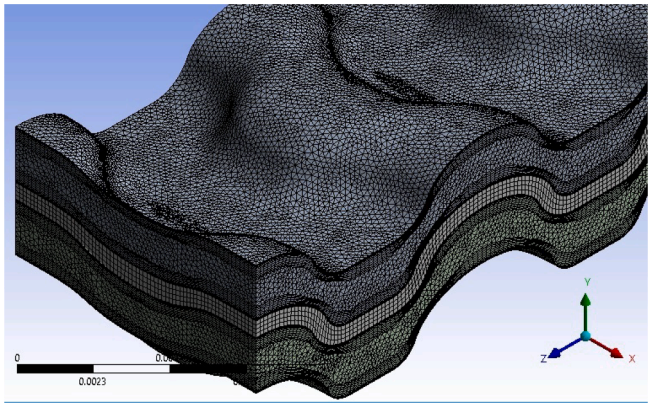

Fig. 4. The meshed geometry for the calculation domain.

performance corresponding to the curve y = tanh (x) is, on average, about 13% greater than the performance corresponding to the closest curve (y = tanh (x/2) [1].

3.2. The influence of the dimensions of the ellipse on the thermal and hydraulic flow characteristics

The average values of the Nusselt number at Reynolds number (500–5000) are calculated from the results of numerical analysis using Eqs. (7) and (8). Fig. 9 shows the average values of Nusselt number

Table 2
Mesh independence test.

	y = tanh(x)	y = tanh(x/3)	(a = 4, b = 1.5) mm	(a = 2.4, b = 2.5)mm
Mesh1	10,886,916	10,884,329	11,999,095	10,103,869
Mesh2	17,926,622	14,825,083	16,692,737	13,468,903
ΔMesh/Mesh1%	64	36	40	33
Δh/h %	2.4 ↓	0.5 ↑	0.5 ↑	2.5 ↓
Δ(ΔP)/ΔP %	1.8 ↓	1.24 ↑	1.9 ↑	2.7 ↑

corresponding to Re numbers according to the corrugation depth of b = 1.5 mm, b = 2 mm, and b = 2.5 mm plate, respectively. Moreover, the Nusselt number corresponding to the plate corrugation depth of b = 2.5 mm is, on average, about 52% greater than the Nusselt number corresponding to the closest case (b = 2 mm) [1]. The increase in the depth of corrugation leads to an increase in the circumference of the heat exchange surface associated with an increase in the longitudinal turbulence of the fluid flow. That is, as the plate corrugation depth increases, the Nusselt number increases [17,16]. Thus, this has to increase the heat exchange between the hot and cold fluids.

Fig. 10 shows the average values of the friction coefficient corresponding to Re numbers for b = 1.5 mm, b = 2 mm, and b = 2.5 mm

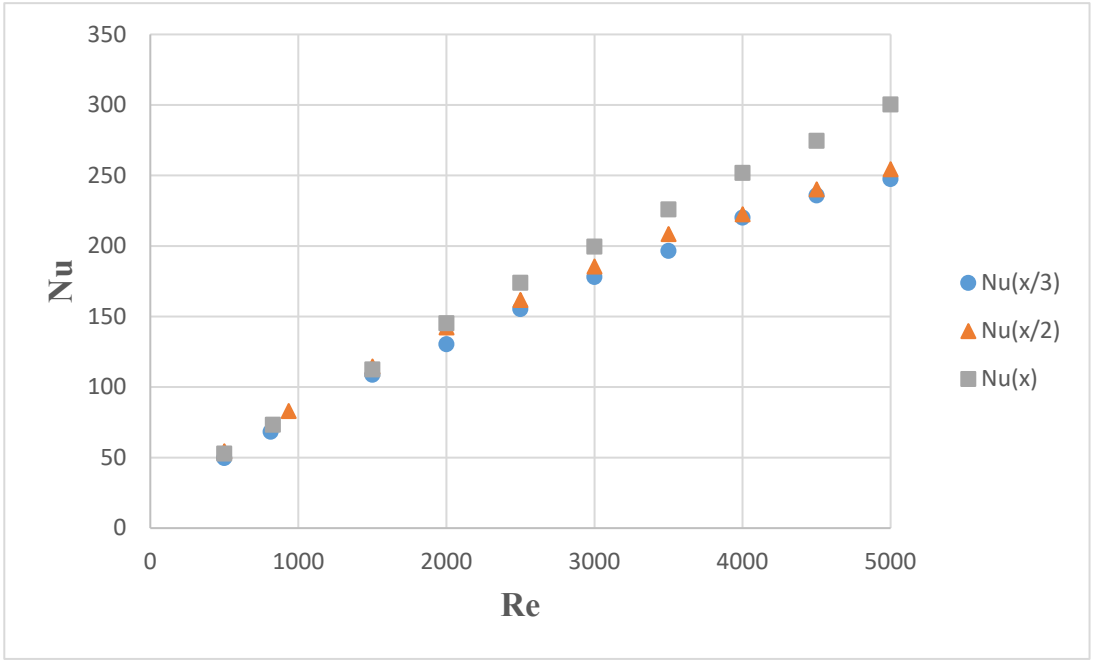

Fig. 5. The average values of the Nusselt number corresponding to the Reynolds numbers according to the functions y = tanh (x), y = tanh (x/2), and y = tanh (x/3) respectively.

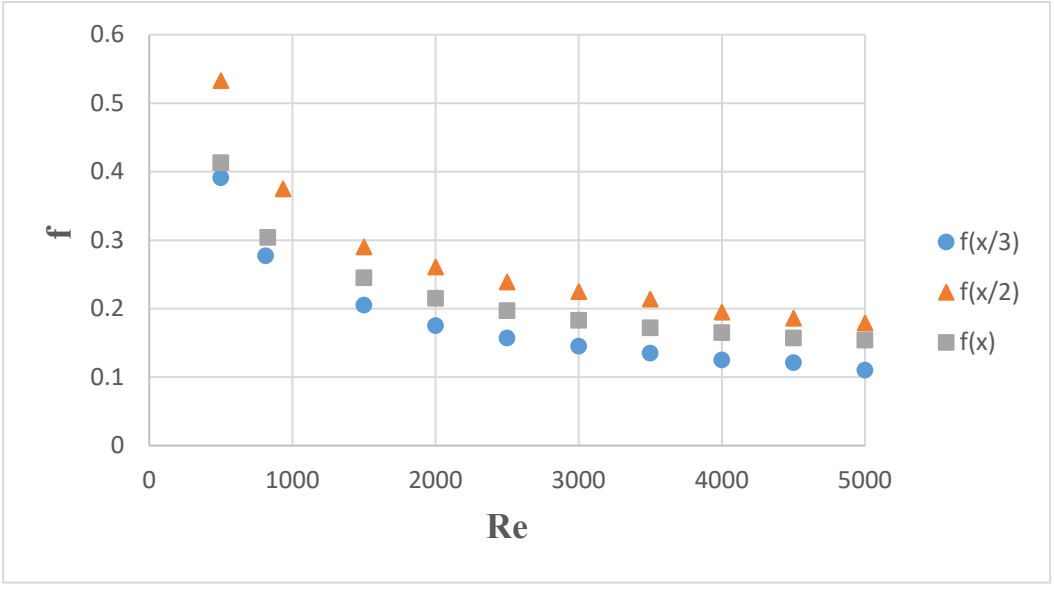

Fig. 6. The average values of the friction coefficient corresponding to Re numbers according to the functions y = tanh (x), y = tanh (x/2), and y = tanh (x/3) respectively.

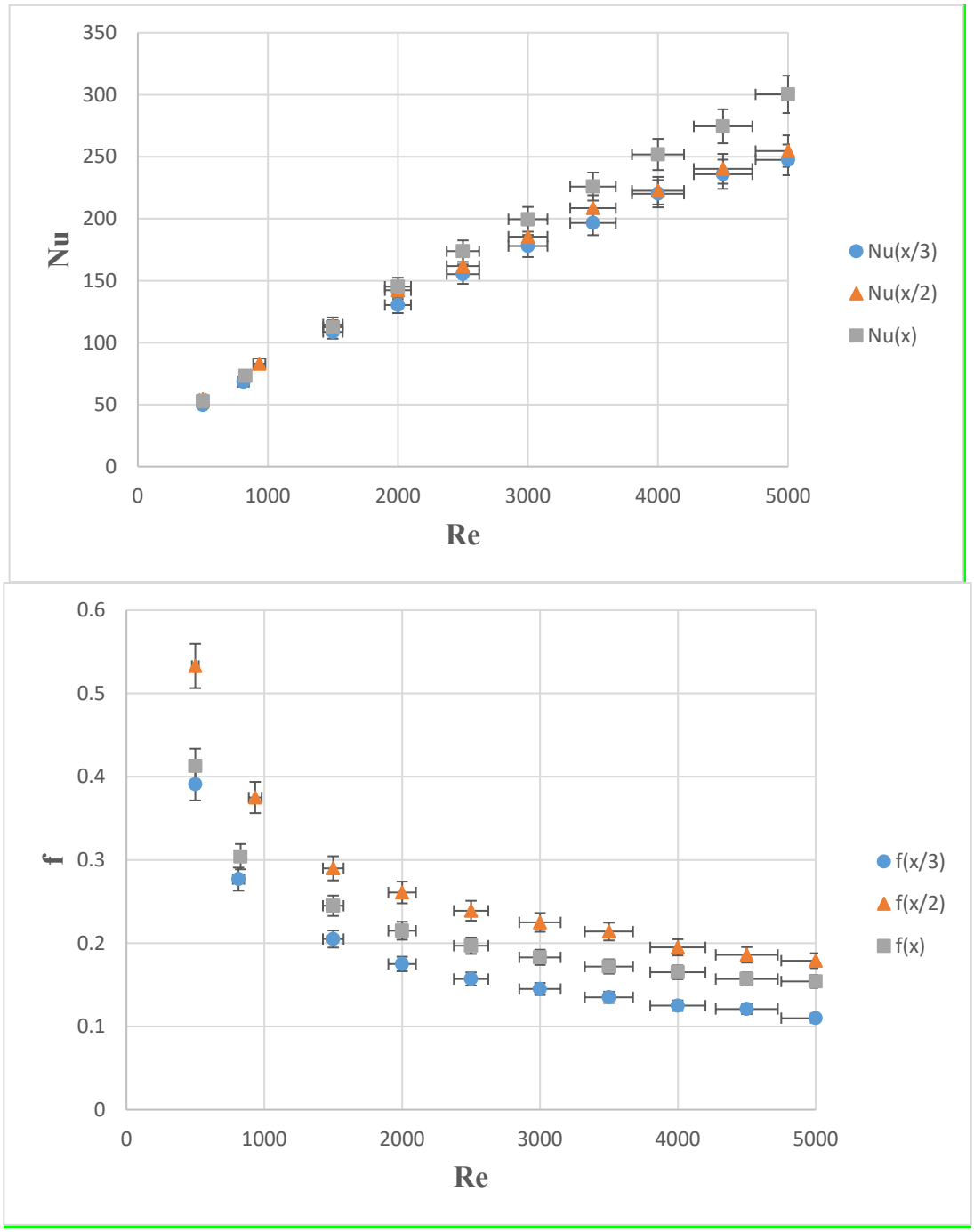

Fig. 7. the error bars for Fig. 5 and Fig. 6, respectively.

plate corrugation depth, respectively. From Fig. 10, it is concluded that the friction coefficient corresponding to the plate corrugation depth of b = 1.5 mm is the lowest when compared with the friction coefficients corresponding to the corrugation depths of the other examined plates. The reduction in corrugation depth reduces the longitudinal fluid turbulence and thus the fluid moves more smoothly due to the lower coefficient of friction.

As for the performance according to the $Nu/f^{1/3}$ parameter, Fig. 11 shows that the flow performance according to the plate corrugation depth of b = 2.5 mm is higher than the performance values of the other 2 examined cases. Where, the performance corresponding to the plate corrugation depth of b = 2.5 mm is, on average, approximately 36% greater than the performance value corresponding to the next closest situation [1].

From a comparison of the results between the effects of the hyperbolic tangent function (transverse turbulence of the fluid) and corrugation depth (longitudinal turbulence of the fluid) on the thermal and hydraulic flow properties, it can be concluded that the effect of longitudinal turbulence on heat exchange and performance is approximately 4 times greater than the effect of transverse turbulence.

The flow models emerging due to the new design of the plate geometry, such as helical, reverse, and furrow flow, play a key role in increasing the mixing of the working fluid in addition to "disturbing" its boundary layer along its path [1]. The study of the effect of changing the

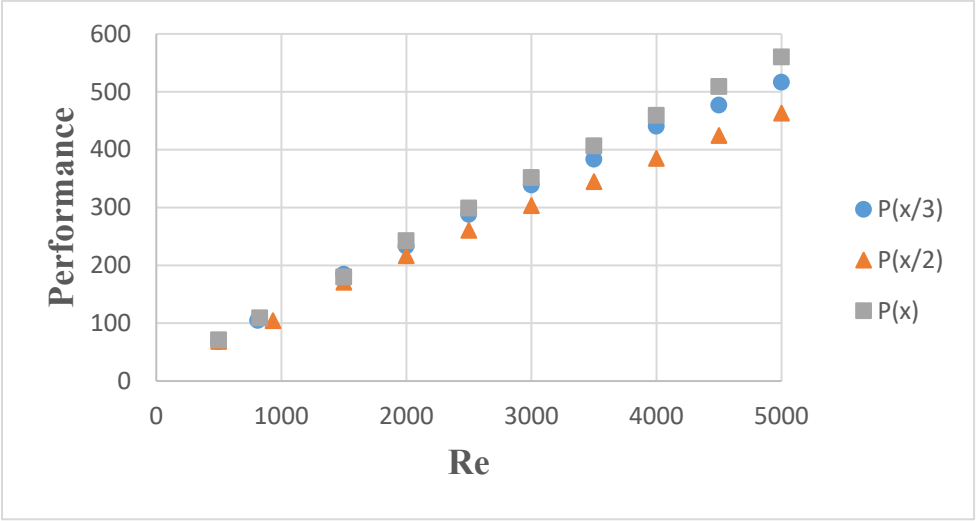

Fig. 8. The average values of the performance ($Nu/f^{1/3}$) corresponding to Re numbers according to the functions y = tanh (x), y = tanh (x/2), and y = tanh (x/3), respectively.

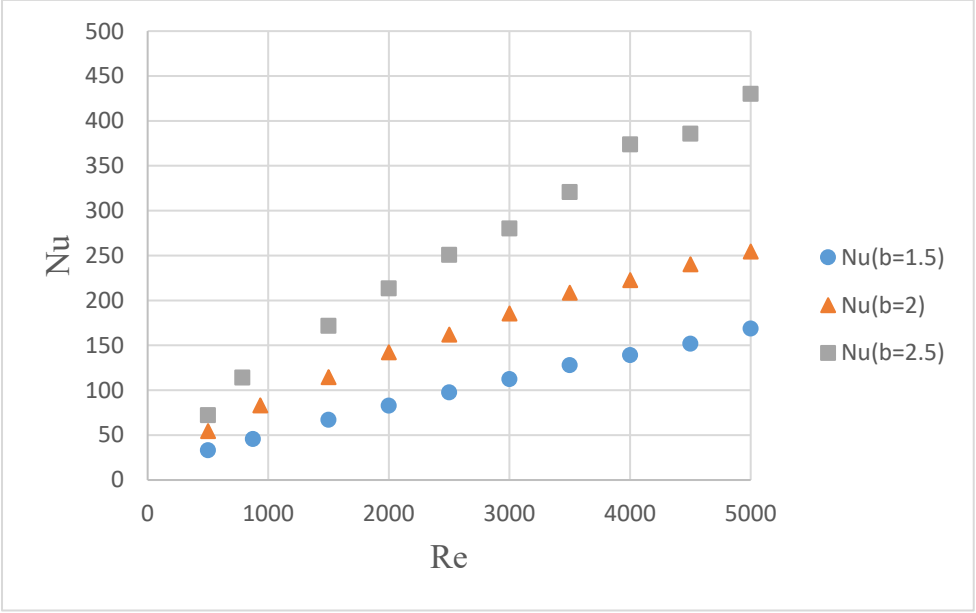

Fig. 9. Average values of Nusselt number corresponding to Re numbers according to the corrugation depth of b = 1.5 mm, b = 2 mm, and b = 2.5 mm plate, respectively.

formula of the hyperbolic function and the depth of ripple on the hydrothermal properties is primarily a study of the effect of these parameters on the mentioned emerging flows, which plays a key role in the increase and decrease of both the Nusselt number and the coefficient of friction. Changing the formula of the hyperbolic tangent function will mainly affect the reverse and furrow flow as it increases with increasing the gradient of the curvature of the function s for changing the ripple depth, the helical flow will mainly be affected and increase with the increase in the ripple depth and thus increase the heat exchange (Nusselt number) and this is consistent with the results of the numerical study (Fig. 5 and Fig. 9).

Here the following question arises: if the ripple is in the transverse and the HTF is in the longitudinal, then will the effect be the same? In other words, if the flow were in the X-axis, what would the effect be? The current lines of flow will run according to the curve of the hyperbolic tangent function and form a zigzag-like flow pattern, and the depth of corrugation will gradually change, significantly reducing the reverse flow pattern, and the furrow flow will prevail more. Thus, this will reduce heat exchange and friction compared to the studied case.

Although it is difficult to compare the performance of PHEs with different plate geometries due to the different range of relationships according to Reynolds numbers, the enhanced performance of NPHE has been compared with those of traditional chevron type plates Kakac and Liu Pramuanjaroenkij [10,12] and new geometrical plates in the literature.

It can be seen from Fig. 12 that the enhanced performance of NPHE outperforms its counterparts with other plate geometry exchangers, with the relative difference being 37% for the closest competitor at the Reynolds number 5000. This superiority can be attributed to the enhancement of the heat transfer by the transverse and longitudinal turbulence of the fluid movement while maintaining a fairly acceptable coefficient of friction compared to other types in which the high heat

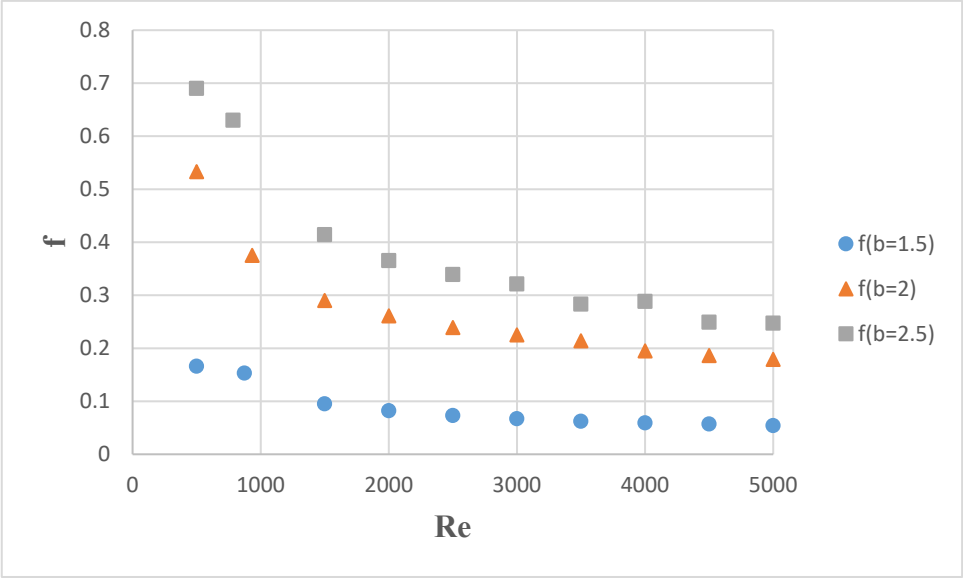

Fig. 10. The average values of the friction coefficient corresponding to Re numbers according to the corrugation depth of the b = 1.5 mm, b = 2 mm, and b = 2.5 mm plate, respectively.

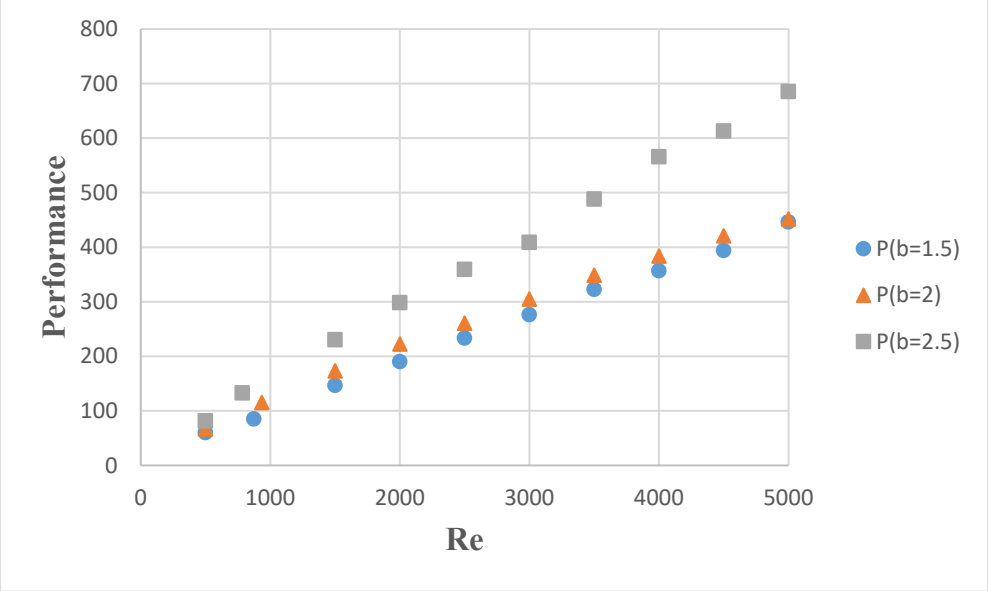

Fig. 11. The average values of the performance corresponding to Re numbers according to the corrugation depth of the b = 1.5 mm, b = 2 mm, and b = 2.5 mm plate, respectively.

transfer is associated with a large coefficient of friction predominates or vice versa.

4. Conclusion

This paper aims to enhance the performance and heat transfer of NPHE by studying numerically the effect of change some geometrical parameters of the novel plate on the flow characteristics. The effect of changing the hyperbolic tangent function HTF and the cross-section dimensions of the plate profile (ellipse) on Nu number, friction coefficient, and Performance was studied. The average values of Nusselt number, friction coefficient, and performance according to the parameter $Nu/f^{1/3}$ were calculated for each of the studied cases within the range of Reynolds number (500–5000). The results showed that the effect of longitudinal turbulences (corrugation depth) on heat transfer and performance was greater than the effect of transverse turbulences (HTF). Where, an improvement in Nusselt number and performance was observed on average by 8% and 13%, respectively, according to the HTF "tanh(x)", while the average improvement of Nusselt number and performance was 52% and 36%, respectively, according to a corrugation depth of 2.5 mm. When comparing the enhanced performance of NPHE with the corresponding performance of conventional chevron type plates and other plates in the literature, a good improvement in performance was found, reaching 37% at Re = 5000. This reflects positively on saving energy and preserving the environment. In future work, the performance and heat transfer of the novel type of this exchanger on the two-phase flow may be studied.

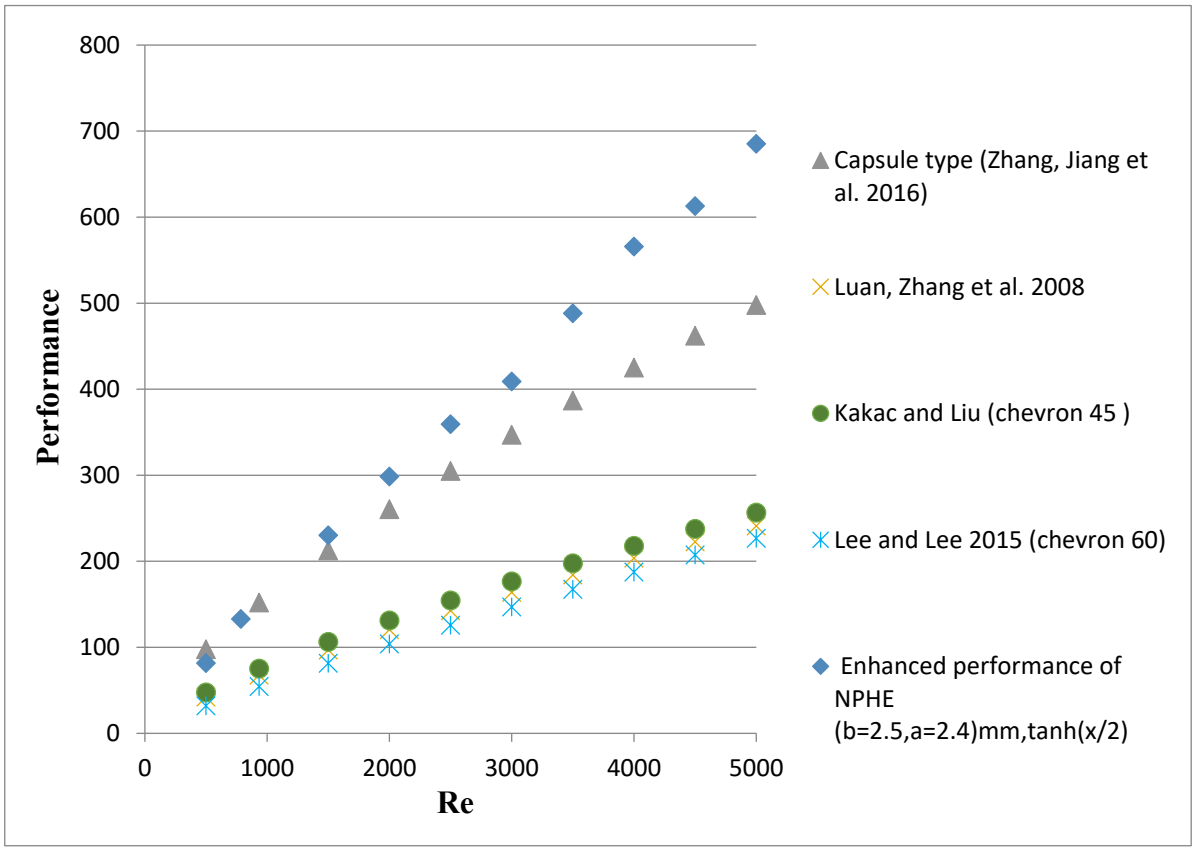

Fig. 12. Comparing the enhanced performance of NPHE with that those of other plates geometries.

CRediT authorship contribution statement

Ahmad Aboul Khail: Conceptualization, Methodology, Software, Validation. **Ali Erişen:** Validation, Supervision.

Declaration of Competing Interest

The authors declare that they have no known competing financial interests or personal relationships that could have appeared to influence the work reported in this paper.

Acknowledgements

This research was supported by scientific research projects coordination unit at KIRIKKALE University under the number 2019/062.

References

[1] A. Aboul Khail, A. Erişen, Improvement of Plate Heat Exchanger Performance Using a New Plate Geometry, Arabian Journal for Science and Engineering. (2021).
[2] F. Afshari, A.D. Tuncer, A. Sözen, H.I. Variyenli, A. Khanlari, E.Y. Gürbüz, A comprehensive survey on utilization of hybrid nanofluid in plate heat exchanger with various number of plates, International Journal of Numerical Methods for Heat & Fluid Flow (2021).
[3] J. Fan, W. Ding, J. Zhang, Y. He, W. Tao, A performance evaluation plot of enhanced heat transfer techniques oriented for energy-saving, International Journal of Heat and Mass Transfer 52 (1–2) (2009) 33–44.
[4] I. Gherasim, N. Galanis, C.T. Nguyen, Heat transfer and fluid flow in a plate heat exchanger. Part II: Assessment of laminar and two-equation turbulent models, International Journal of Thermal Sciences 50 (8) (2011) 1499–1511.
[5] O. Giurgiu, A. Pleşa, L. Socaciu, Plate heat exchangers–flow analysis through mini channels, Energy Procedia 85 (2016) 244–251.
[6] M.S. Islam, S.C. Saha, Heat transfer augmentation in retrofitted corrugated plate heat exchanger, International Journal of Heat and Mass Transfer 161 (2020), 120226.
[7] M.S. Islam, S.C. Saha, Heat transfer enhancement investigation in a novel flat plate heat exchanger, International Journal of Thermal Sciences 161 (2021), 106763.
[8] M.S. Islam, S.C. Saha, Heat transfer enhancement of modified flat plate heat exchanger, Applied Thermal Engineering 186 (2021), 116533.
[9] M.S. Islam, F. Xu, S.C. Saha, Thermal performance investigation in a novel corrugated plate heat exchanger, International journal of heat and mass transfer 148 (2020), 119095.
[10] Kakac, S. and H. Liu Pramuanjaroenkij. 2012. Heat exchangers: selection, rating, and thermal design. CRC Press, Taylor & Francis Group, Florida, US.
[11] A.G. Kanaris, A.A. Mouza, S.V. Paras, Flow and heat transfer prediction in a corrugated plate heat exchanger using a CFD code, Chemical Engineering & Technology: Industrial Chemistry-Plant Equipment-Process Engineering-Biotechnology 29 (8) (2006) 923–930.
[12] J. Lee, K.-S. Lee, Friction and Colburn factor correlations and shape optimization of chevron-type plate heat exchangers, Applied Thermal Engineering 89 (2015) 62–69.
[13] W. Li, H.-X. Li, G.-Q. Li, S.-C. Yao, Numerical and experimental analysis of composite fouling in corrugated plate heat exchangers, International Journal of heat and mass transfer 63 (2013) 351–360.
[14] Z.-J. Luan, G.-M. Zhang, M.-C. Tian, M.-X. Fan, Flow resistance and heat transfer characteristics of a new-type plate heat exchanger, Journal of Hydrodynamics 20 (4) (2008) 524–529.
[15] Matsegora, O. I., J. J. Klemeš, O. P. Arsenyeva, P. O. Kapustenko, S. K. Kusakov and V. V. Zorenko (2019). "The effect of plate corrugations geometry on performance of plate heat exchangers subjected to fouling.".
[16] S. Mohebbi, F. Veysi, Numerical investigation of small plate heat exchangers performance having different surface profiles, Applied Thermal Engineering 188 (2021), 116616.
[17] Mohebbi, S. and F. J. A. T. E. Veysi (2021). "Numerical investigation of small plate heat exchangers performance having different surface profiles." **188**. 116616.
[18] H. Shokouhmand, M. Hasanpour, Effect of number of plates on the thermal performance of a plate heat exchanger with considering flow maldistribution, Journal of Energy Storage 32 (2020), 101907.
[19] Y.-N. Wang, J.-P. Lee, M.-H. Park, B.-J. Jin, T.-J. Yun, Y.-H. Song, I.-S. Kim, A study on 3D numerical model for plate heat exchanger, Procedia engineering 174 (2017) 188–194.
[20] L. Zhang, D. Che, Influence of corrugation profile on the thermalhydraulic performance of cross-corrugated plates, Numerical Heat Transfer, Part A: Applications 59 (4) (2011) 267–296.
[21] Y. Zhang, C. Jiang, Z. Yang, Y. Zhang, B. Bai, Numerical study on heat transfer enhancement in capsule-type plate heat exchangers, Applied Thermal Engineering 108 (2016) 1237–1242.